

Electronic Supplementary Information

**Electric field assisted assembly of 1D supramolecular nanofibres for enhanced supercapacitive performance**

Suman Kundu,<sup>ab</sup> Subi J. George<sup>c</sup> and Giridhar U. Kulkarni<sup>\*d</sup>

<sup>a</sup> Centre for Nano and Soft Matter Sciences, Jalahalli, Bangalore 560013, India

<sup>b</sup> Manipal Academy of Higher Education, Manipal 576104, India

<sup>c</sup> Supramolecular Chemistry Laboratory, New Chemistry Unit, Jawaharlal Nehru Centre for Advanced Scientific Research, Bangalore 560064, India

<sup>d</sup> Chemistry and Physics of Materials Unit, Jawaharlal Nehru Centre for Advanced Scientific Research, Jakkur, Bangalore, India

\* Corresponding author.

E-mail address: kulkarni@jncastr.ac.in

**Table T1.** Examples of the devices made by dielectrophoresis alignment of 1D nano-objects for different applications as mentioned in the table.

Sl. No.	Reference	Material used for the alignment	Application
1	Solid State Communications 148 (2008) 194–198	GaN NWs	UV sensor
2	Nanotechnology 17 (2006) 2567–2573	ZnO nanowire	UV sensor
3	J. Phys. D: Appl. Phys. 36 (2003) L109–L114	CNT	Ammonia sensing
4	Sensors and Actuators B 105 (2005) 164–169	CNT	HF, SO <sub>2</sub> sensing
5	Sensors and Actuators B 108 (2005) 398–403	CNT	NO <sub>2</sub> sensing
6	Sensors and Actuators B 114 (2006) 943–949	CNT	NO <sub>2</sub> sensing
7	Sensors and Actuators B 125 (2007) 55–59	PEDOT/PSS nanowires	Acetone, methanol and ethanol sensing
8	JOURNAL OF APPLIED PHYSICS 101, 073704, 2007	CdSe nanowires	Field-enhanced emission
9	APPLIED PHYSICS LETTERS 90, 043104, 2007	Gallium nitride nanowire	FET
10	Nature Nanotechnology volume 3, pages 88–92(2008)	Silicon and rhodium nanowires	Resonator array
11	Procedia Chemistry 1 (2009) 947–950	ZnO nanorods	CO sensing
12	Nanotechnology 22 (2011) 105602 (8pp)	poly(9,9-dioctylfluorene) nanofibre	polarized light emission
13	ACS Appl. Mater. Interfaces 2017, 9, 22837–22845	Ag Nanowire–ZnO-Branched Nanorod	UV sensor
14	ACS Appl. Mater. Interfaces 2017, 9, 37912–37920	p/MQW/n InGaN Nanorod	LED
15	IEEE Transactions On Nanotechnology, Vol. 7, No. 6, November 2008	GaN Nanowires	MESFET
16	J. Appl. Phys. 100, 114310 (2006)	GaN nanowire	FET
17	Sensors and Actuators B 239 (2017) 358–363	zinc oxide nanowires	H <sub>2</sub> S sensing
18	ACS Appl. Mater. Interfaces 2015, 7, 12713–12718	Au/ZnO nanowires	UV sensor
19	Sensors and Actuators B: Chemical, Volume 194, 2014, Pages 1-9	TiO <sub>2</sub> Nanowires	NH <sub>3</sub> , acetone, and ethanol sensing
20	Nanotechnology 30 (2019) 105706 (10pp)	InAs nanowires	NO <sub>2</sub> sensing
21	Appl. Phys. A 87, 739–742	GaN nanowire	Half-wave rectifier

	(2007)		
22	Chin J Anal Chem, 2012, 40(1), 145–149	CNT	NH <sub>3</sub> sensing
23	Nanotechnology 30 (2019) 475202 (9pp)	Ag nanowire	SERS
24	Sensors and Actuators B 127 (2007) 505–511	CNT/Pd	H <sub>2</sub> sensing
25	J Mater Sci: Mater Electron (2013) 24:4554–4559	Se nanorods	UV sensor
26	Phys. Scr. 90 (2015) 094017 (4pp)	Bi <sub>2</sub> S <sub>3</sub> nanowire	Humidity sensing
27	Sensors and Actuators B 221 (2015) 104–112	SnO <sub>2</sub> , ZnO, TiO <sub>2</sub> nanowires	Photosensor, CO sensor, FET
28	Sensors and Actuators B 166–167 (2012) 12–16	ZnO nanowires	UV sensor
29	CARBON 94 (2015) 911–918	CDC–MWCNT	Electrochemical capacitor
30	ACS Nano 2009, 3, 11, 3679–3683	CNTs	Electrochemical capacitor

**Note: Parameters optimised for randomly oriented nanofibres device**

To arrive at the optimised device performance, both the concentration and ageing of the nanofibre solution have been tried out during fabrication. At first, we prepared 8mM CS-DMV stock solution following the synthesis method as described in the experimental section. The desired concentration of the CS-DMV nanofibre solution was then prepared by adding an appropriate amount of deionized water. At lower concentrations (1-10  $\mu$ M), the nanofibres did not seem to get formed (see Figure S1). The nanofibres growth was seen at concentrations higher than 50  $\mu$ M. The optimal concentration was found to be around  $\sim$  0.5 mM for attaining well-formed nanofibres. At even higher concentrations, the nanofibres get agglomerated as seen under the optical microscope.

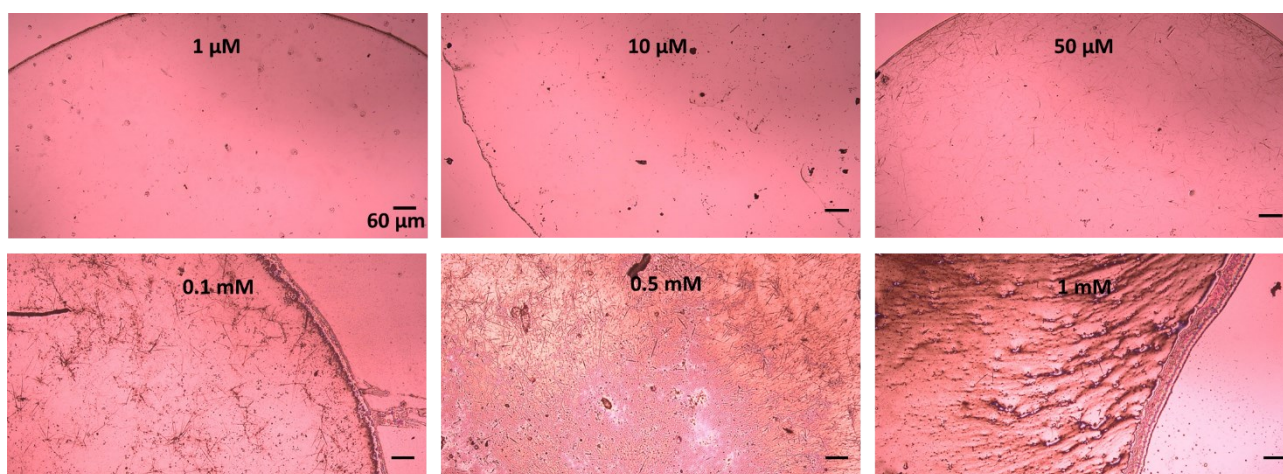


Figure S1. Optical microscopic images of 1 $\mu$ L volume of CS-DMV solution (1 week old) drop cast on Ti/Glass. The concentration of the CS-DMV solutions varied as indicated on top of each figure.

We have also found that the prepared CS-DMV solutions required a duration of 1 week of ageing to produce well formed nanofibres in the dispersion (see Figure S2).

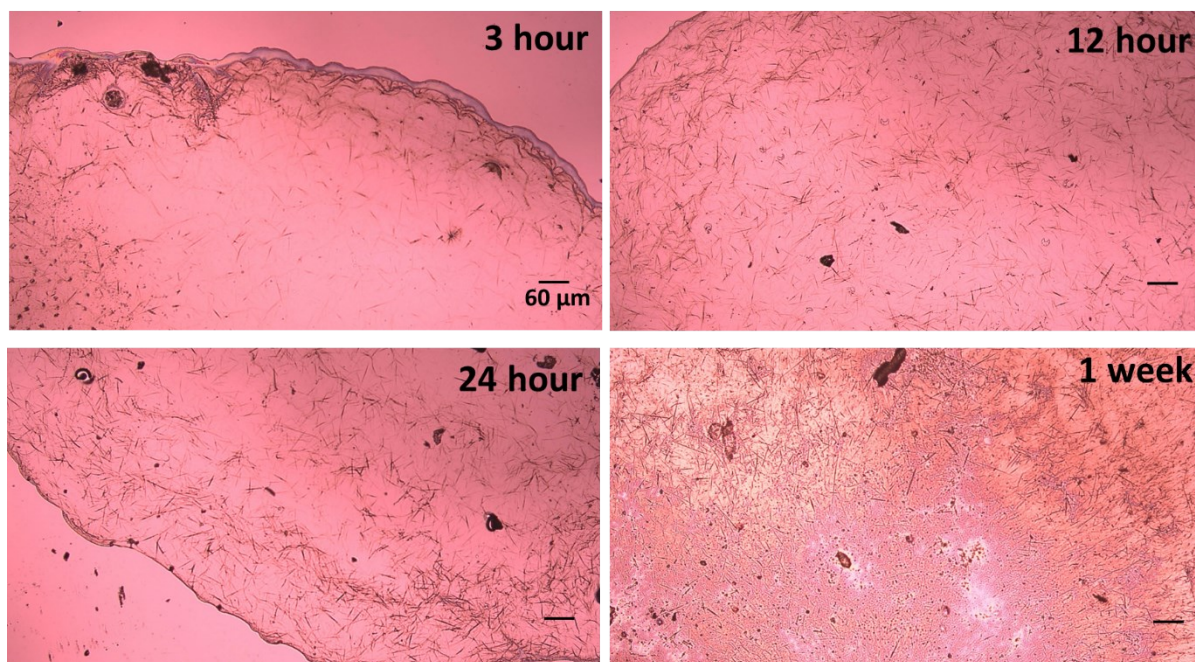


Figure S2. Optical microscopic images of 1 $\mu$ L volume of 0.5 mM CS-DMV solution drop cast on Ti/Glass. The time after preparing the fresh CS-DMV solution indicated on top of each figure.

The parameters optimised with respect to the composition of the electrode and the width of the microgap have been detailed out in our previous work.<sup>1</sup>

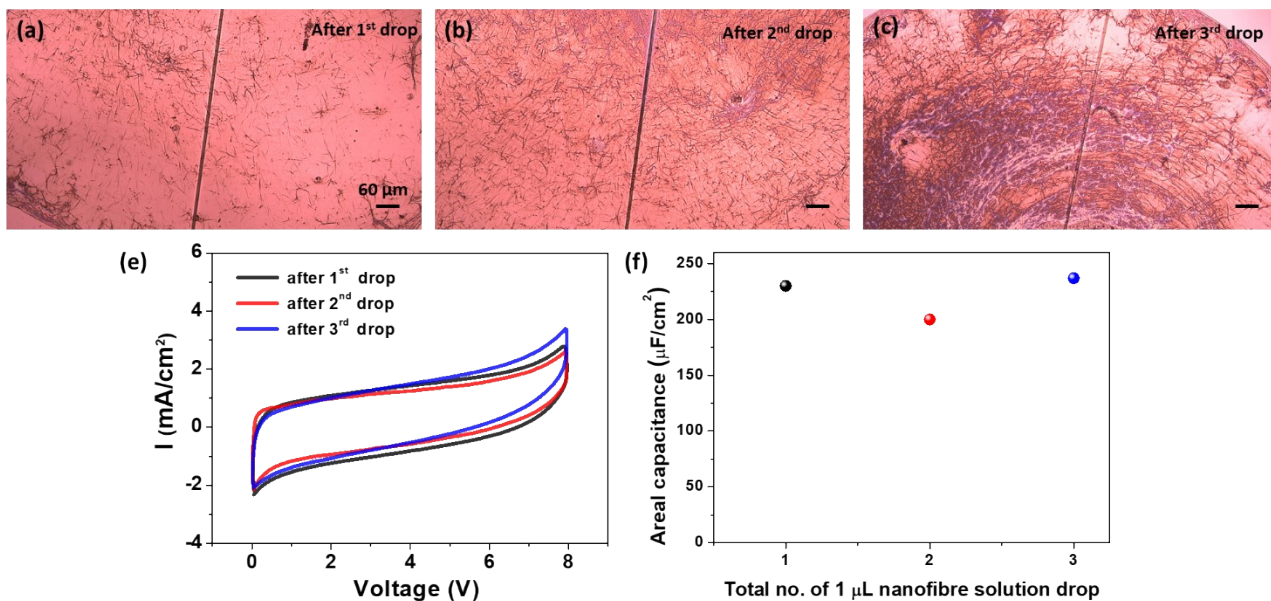


Figure S3. Optical microscope images of the device after putting (a) first (b) second and (c) third drop of nanofibre solution on the same place. Each drop consists of 1 μL of 0.5 mM nanofibre dispersion. (e) Cyclic voltammetry of the devices shown in (a) to (c). (f) Areal capacitances calculated from (e), indicating nominal improvement in the device performance with increasing number of nanofibre drops.

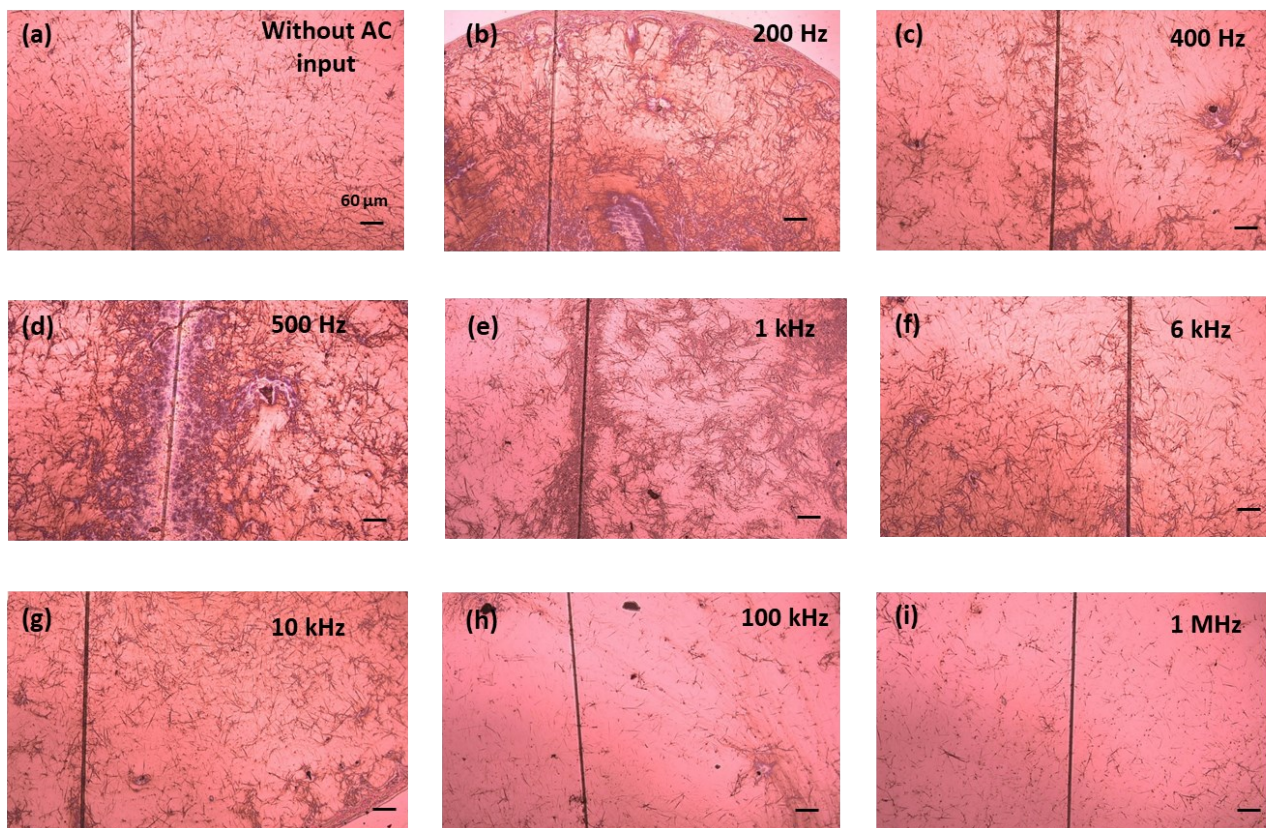


Figure S4. Optical microscope images showing the formation of nanofibre mat along the gap with applying AC input of various frequencies. Here, AC peak to peak voltage fixed at 2 V.

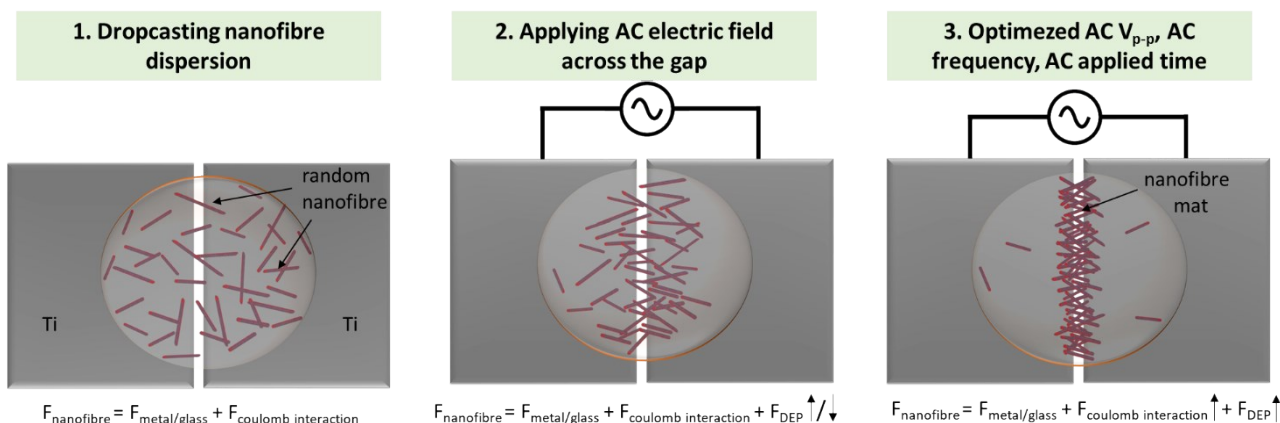


Figure S5. Schematic of random nanofibres to nanofibre mat formation. 1. Simply drop-casting the nanofibre dispersion would result in randomly oriented nanofibres on top of the Ti electrodes. Here, the forces acting on a single nanofibre ( $F_{\text{nanofibre}}$ ) are  $F_{\text{metal/glass}}$  which arises from the electrostatic interaction between the nanofibre and below electrode/substrate and  $F_{\text{coulomb interaction}}$ , coulombic interaction with the adjacent nanofibres. As in this condition, the nanofibres are randomly oriented the  $F_{\text{coulomb interaction}}$  will be low. 2. While the introduction of an AC electric field will result in additional dielectrophoresis force ( $F_{\text{DEP}}$ ) on the nanofibre. 3. Further, applying AC electric field with the optimised input voltage, frequency and time will result in aligning the nanofibres along the gap. Once the initial nanofibres deposited along the gap, the electric field around them modifies and the further nanofibres get aligned according to the modified electric field.<sup>2</sup> The magnitude of  $F_{\text{coulomb interaction}}$  will be very high in this case as the nanofibres are very closer to each other and they may form bundles with each other and further the formation of nanofibre mat would follow.

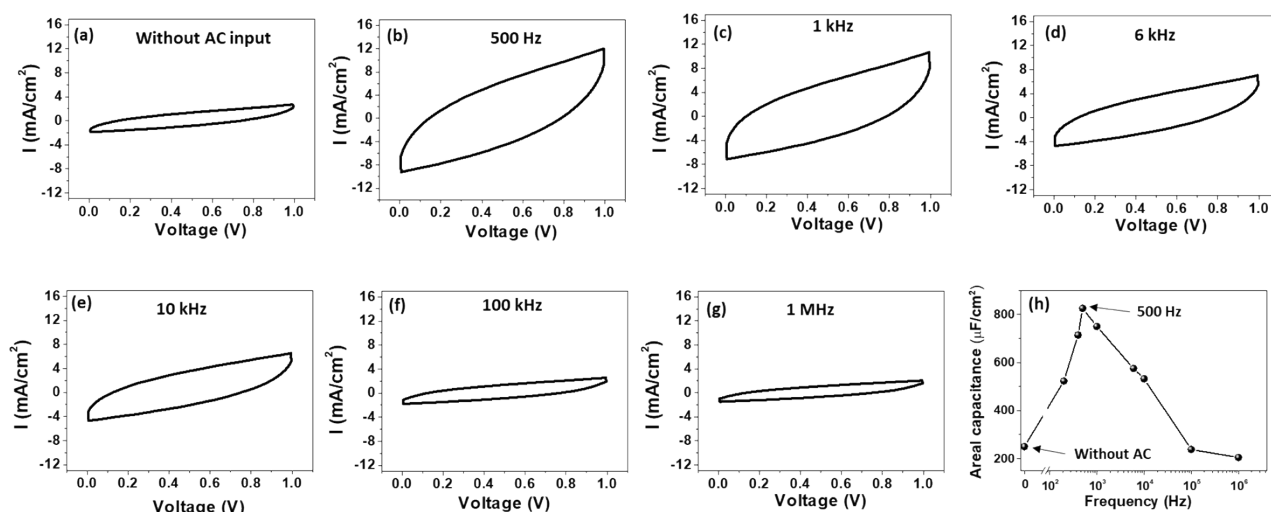


Figure S6. (a-g) Cyclic voltammetry curves of the devices made with applying AC input with various frequencies. AC peak to peak input voltage fixed at 2 V. (h) Areal capacitance values for the devices made with varying AC input frequencies.

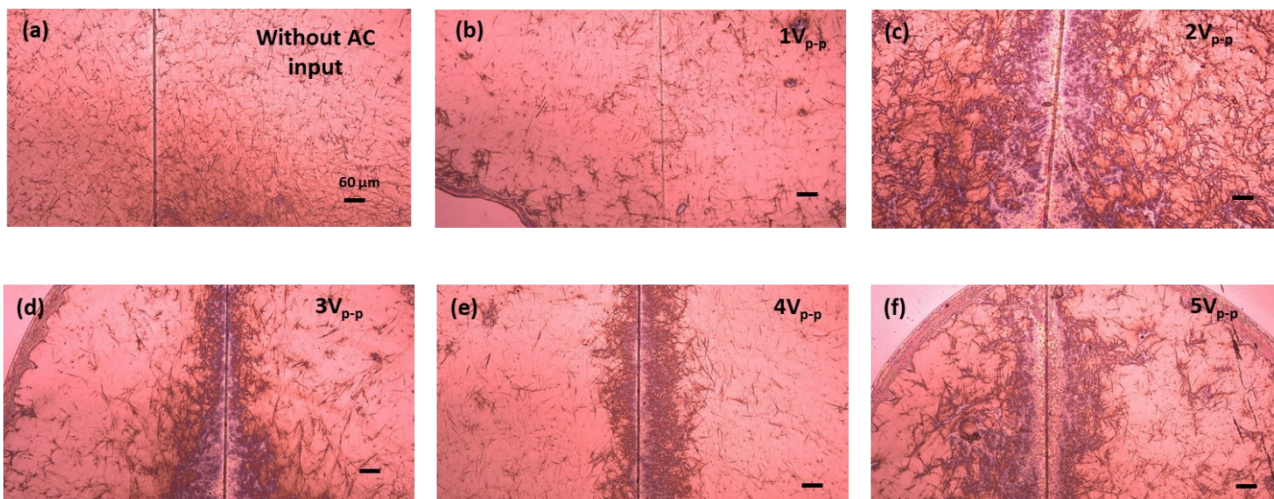


Figure S7. Optical microscope images showing the formation of nanofibre mat along the gap with applying different AC peak to peak input voltages as indicated inside the figures. Here, the AC input frequency fixed at 500 Hz.

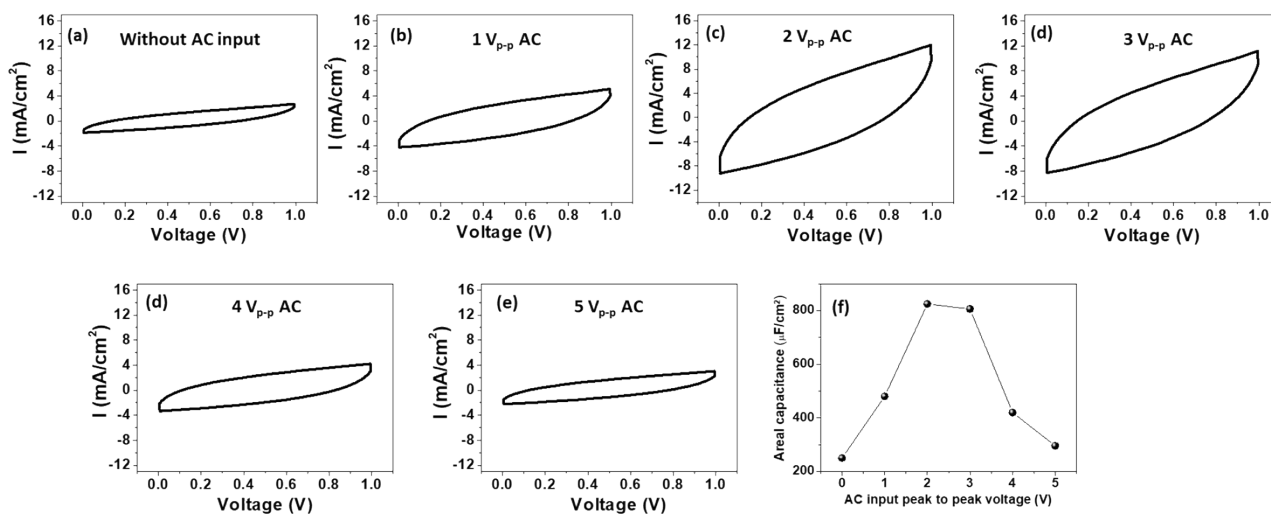


Figure S8. Cyclic voltammetry curves of the devices made with different AC peak to peak input voltage as indicated inside the figures. AC input frequency fixed at 500 Hz. The CV curves acquired at a scan rate of 10V/s. (f) The areal capacitance values for the devices calculated from (a-e).

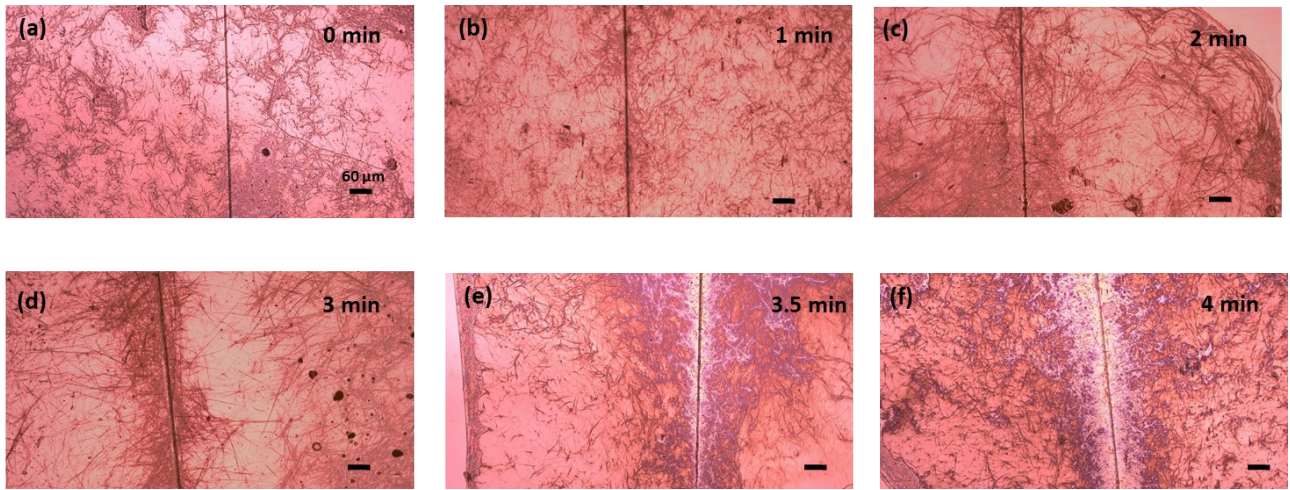


Figure S9. Optical microscope images showing the formation of nanofibre mat along the gap with applying AC input for varied time: 0-4 min. Here, AC peak to peak input voltage and frequency fixed at 2 V and 500 Hz.

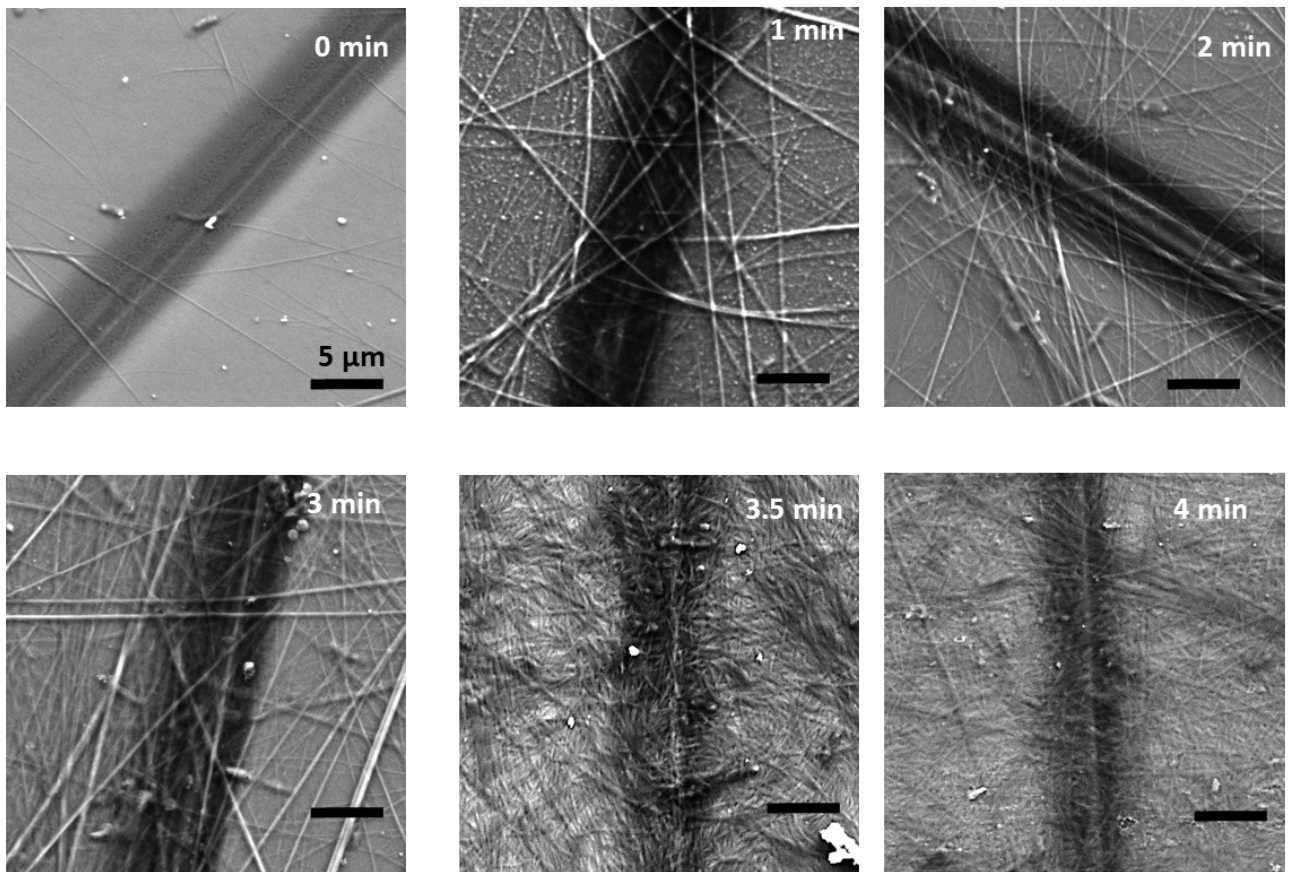


Figure S10. FESEM images showing the formation of nanofibre mat along the gap with applying AC input for varied time: 0-4 min. Here, AC peak to peak input voltage and frequency fixed at 2 V and 500 Hz.

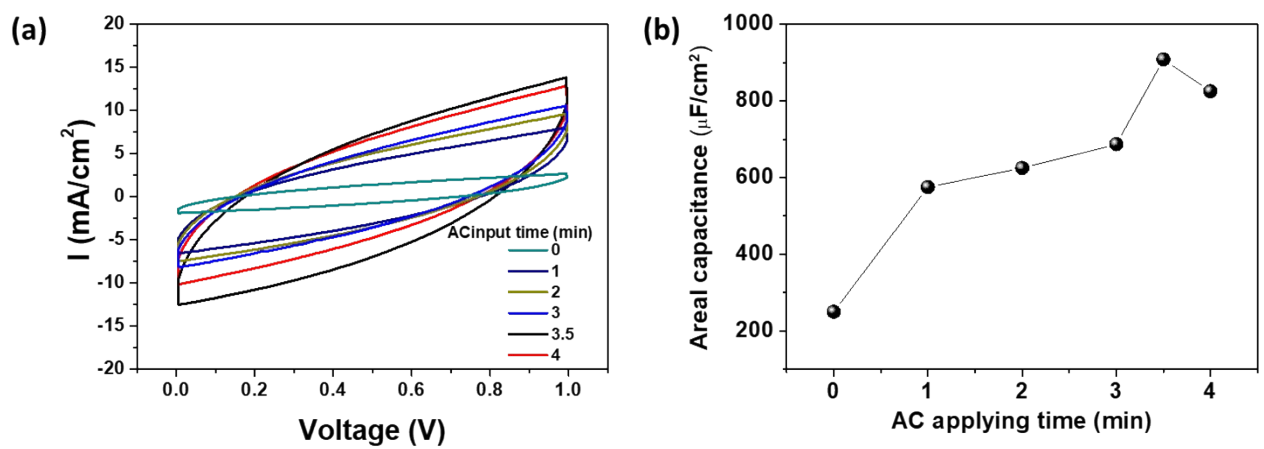


Figure S11. Cyclic voltammety curves of the devices made with applying AC input for varied time: 0-4 min, as indicated inside the figure. AC peak to peak input voltage and frequency fixed at 2 V and 500 Hz.

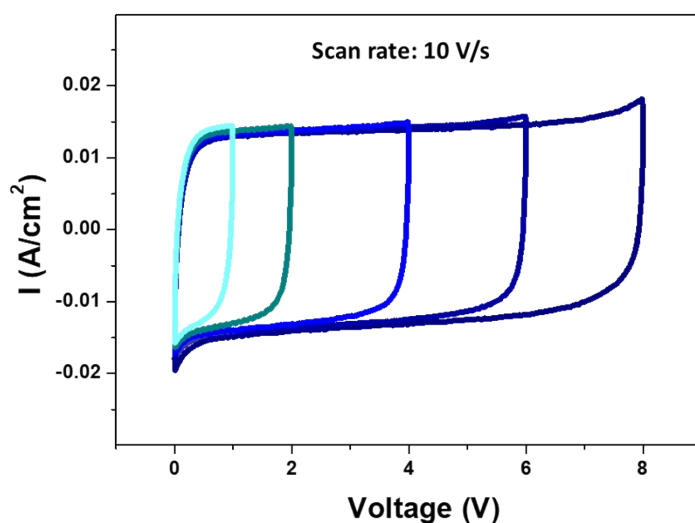


Figure S12. Cyclic voltammety curves of the devices made with applying AC input 3.5 minutes, measured at increasing voltage windows (0-1 to 0-8 V) at 10 V/s scan rate. AC peak to peak input voltage and frequency fixed at 2 V and 500 Hz.

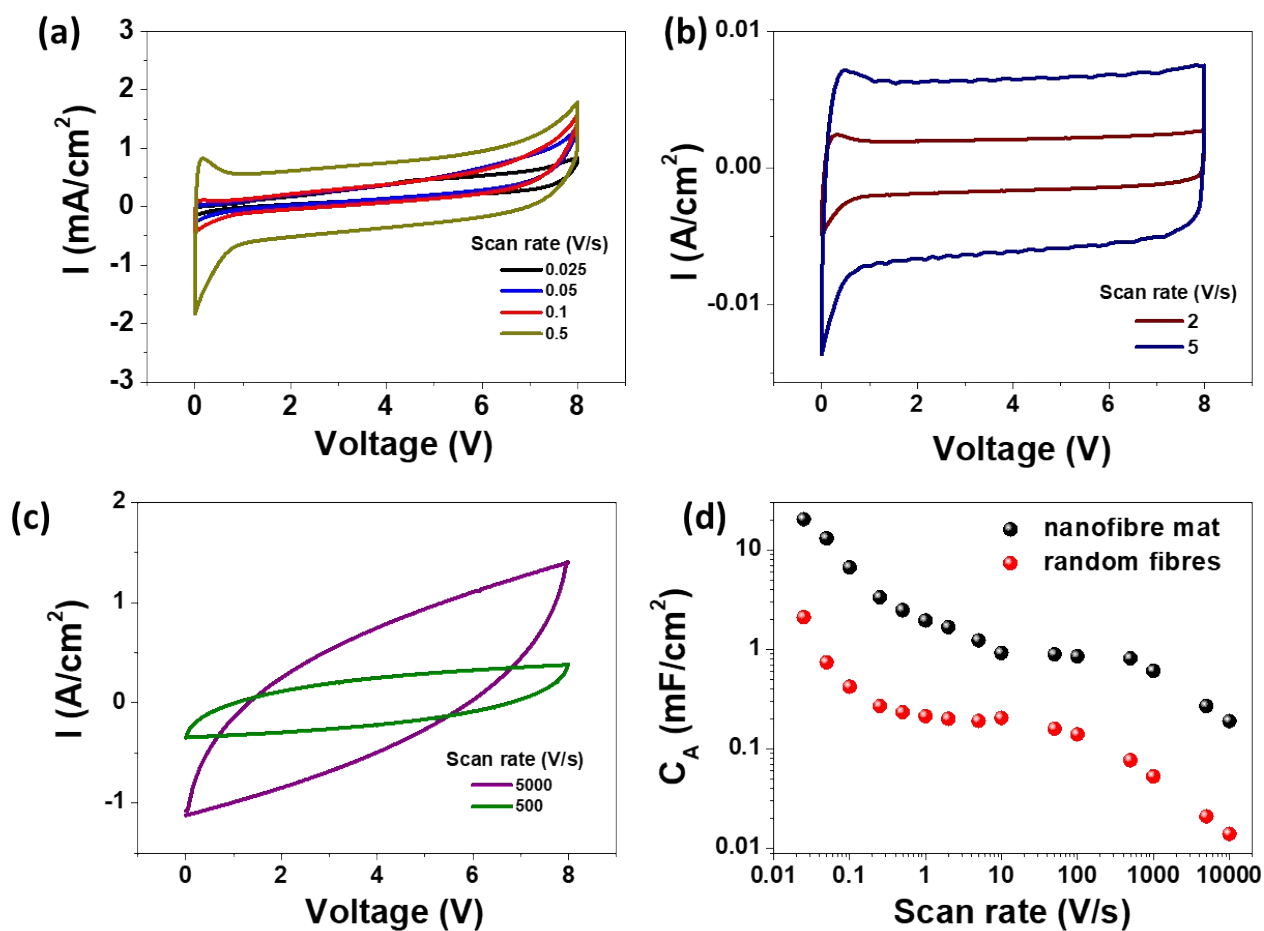


Figure S13. Cyclic voltammetry curves of the device made with nanofibre mat at 0 – 8 V for different scan rates are shown in (a) - (c). The areal capacitance values in logarithmic scale different scan rates calculated for the devices made with random and aligned fibres are shown in (d).

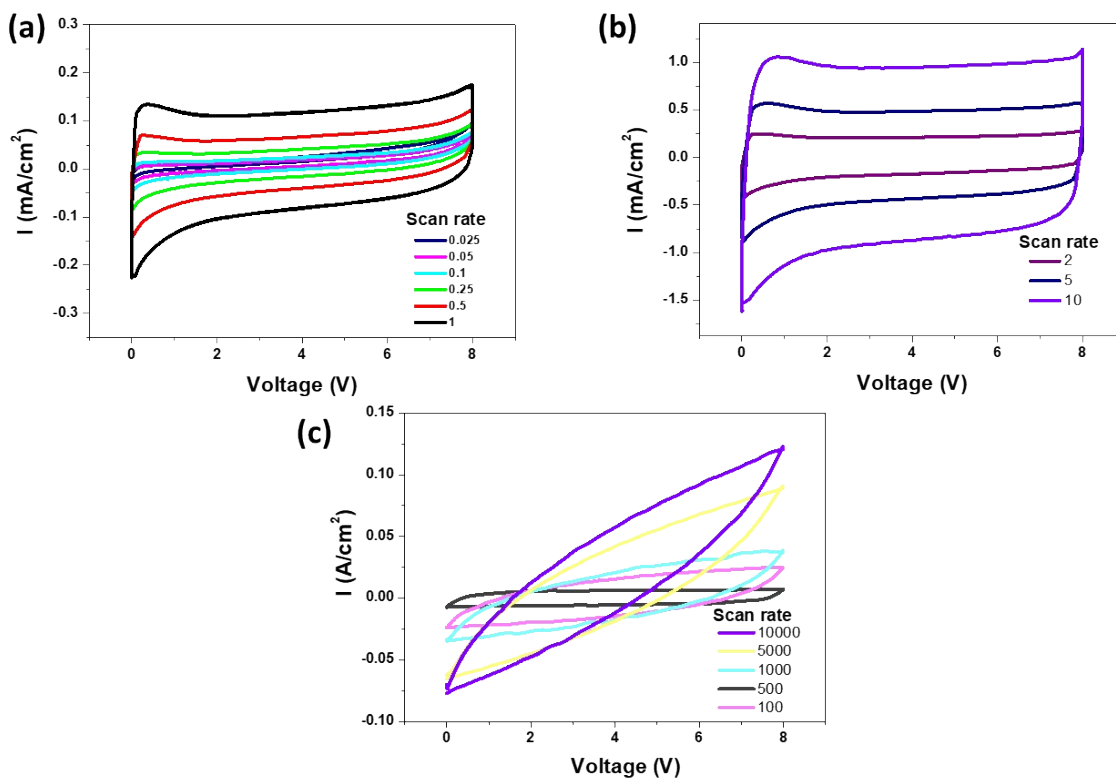
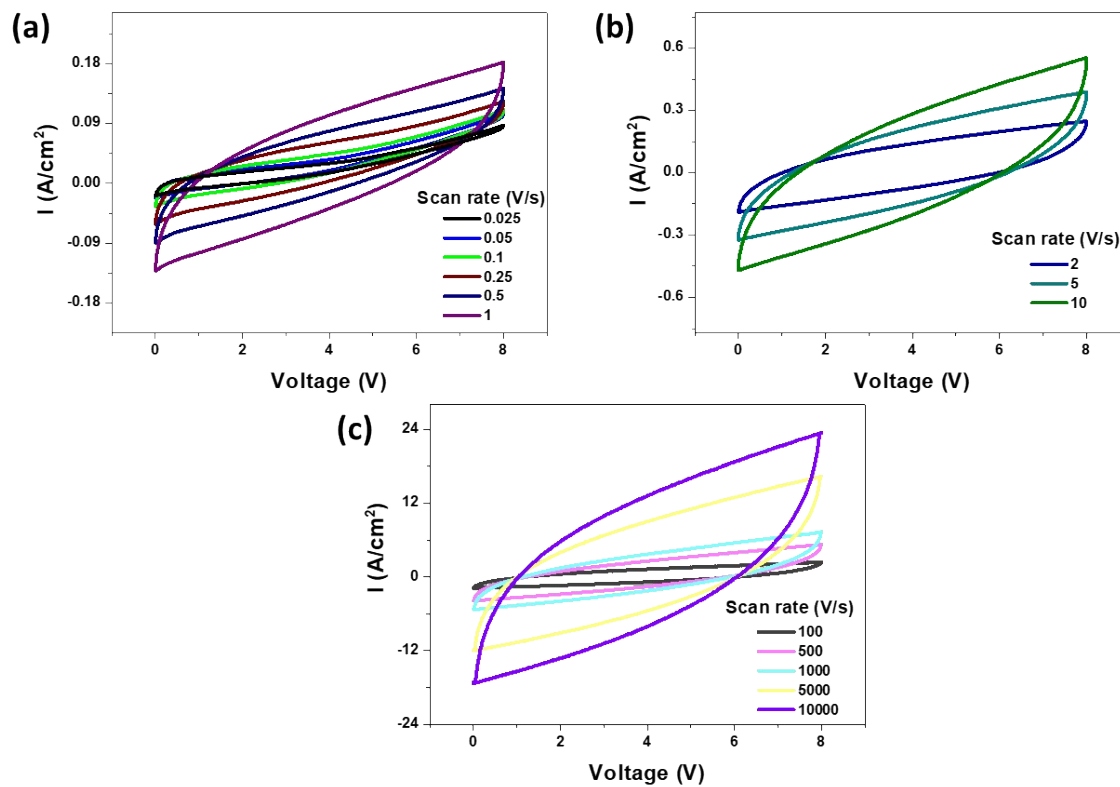


Figure S14. Cyclic voltammetry curves of the device made with random nanofibres at 0 – 8 V



for different scan rates.

Figure S15. Cyclic voltammetry curves of the device made with nanofibre mat in the presence of KBr crystallites, and high humidity (90 %RH) at a potential window of 0 – 8 V for different scan rates.

References:

1. S. Kundu, U. Mogera, S. J. George and G. U. Kulkarni, *Nano Energy*, 2019, **61**, 259-266
2. Y. Liu, J. H. Chung, W. K. Liu and R. S. Ruoff, *J. Phys. Chem. B*, 2006, **110**, 14098-14106.